

# TECHNICAL PHYSICS

Founded by Ioffe Institute

Published since January 1931, 12 issues annually

Editor-in-Chief: Andrei G. Zabrodskii

## Editorial Board:

Alexander A. Schmidt (Deputy Editor-in-Chief), Evgenii B. Aleksandrov, Andrei N. Aleshin, Sergey V. Bobashev, Alexander V. Bobyl, Grigory G. Denisov, Mikhail I. Dyakonov, Nikolai N. Gorelenkov, Viktor V. Gusarov, Aleksandra M. Kalashnikova, Elena S. Kornilova, Alexander V. Kozlov, Zakhary F. Krasilnik, Anatolii V. Krasilnikov, Vladimir E. Kurochkin, Elena V. Kustova, Viktor I. Kuznetsov, Sergey V. Lebedev, Svyatoslav V. Medvedev, Alexey V. Nashchekin, Vadimir I. Nilolaev, Nikolay A. Poklonski, Yuriy A. Rezunkov, Anatoliy M. Shalagin, Mikhail L. Shmatov, German A. Shneerson, Leonid I. Shmaenok, Georgii V. Skornyakov, Evgeny M. Smirnov, Grigorii S. Sokolovskii, Robert A. Suris, Sergey A. Tarasenko, Valerii V. Tuchin, Vladimir V. Ustinov, Anton K. Vershovskii

*ISSN: 1063-7842 (print), 1090-6525 (online)*

TECHNICAL PHYSICS is the English translation of ЖУРНАЛ ТЕХНИЧЕСКОЙ ФИЗИКИ (ZHURNAL TEKHNICHESKOI FIZIKI)

Published by Ioffe Institute

02

## Exploring electron-energetic properties of composite films based on graphene, $\text{LiTi}_2(\text{PO}_4)_3$ and $\text{Li}_3\text{V}_2(\text{PO}_4)_3$ by first-principle methods

© V.V. Shunaev,<sup>1</sup> A.A. Petrunin,<sup>1</sup> A.V. Ushakov,<sup>1</sup> O.E. Glukhova<sup>1,2</sup>

<sup>1</sup> Saratov National Research State University,  
410012 Saratov, Russia

<sup>2</sup> I.M. Sechenov First Moscow State Medical University,  
119048 Moscow, Russia  
e-mail: vshunaev@list.ru

Received April 7, 2025

Revised June 23, 2025

Accepted June 30, 2025

By the density functional theory method, supercells of composite films based on graphene, lithium-titanium phosphate and vanadium-lithium phosphate with different types of stacking were constructed. It was found that the mutual arrangement of the components significantly affects the electron-energy parameters of these structures. The obtained results contribute to solving the experimental problem of improving the performance and energy efficiency of lithium-ion batteries, in which the considered structures can be used as cathodes.

**Keywords:** graphene, lithium titanium phosphate, vanadium lithium phosphate, quantum capacitance, surface charge, density of state.

DOI: 10.61011/TP.2026.01.62836.57-25

### Introduction

One of the relevant scientific challenges in the power field is a search for and development of new effective and durable materials that can act as electrodes for chemical current sources. Lithium-vanadium phosphate  $\text{Li}_3\text{V}_2(\text{PO}_4)_3$  (LVP) is a promising cathode material for fast-charging accumulators [1,2]. Lithium-titanium phosphate  $\text{LiTi}_2(\text{PO}_4)_3$  (LTP) is a good base for solid-phase accumulator electrolyte [3], and at the same time it can act as an anode material [4] or an additive to the cathode material with LVP for monitoring side processes [5]. Rhombohedral LTP and monoclinic LVP belong to a NASICON group of superionic conductors and their structural specific features facilitate easy diffusion of lithium ions [3]. It is reported that the lithium-ion accumulators, in which LTP and LVP act as the anode and the cathode, respectively, maintain high charge/discharge rates and performance of their components as well as demonstrate high cyclic stability even at low temperatures [6,7]. However, LTP and LVP have low conductivity and lose mechanical stability during charging/discharging. Covering particles of these materials with a carbon coating or formation of other LTP or LVP electrode composites with particles of carbon nanomaterials contributes to an increase of electron conduction and mechanical strength of the electrode [8,9]. At the same time, we still do not investigate an issue of interaction of phosphates between each other and with nanocarbon structures at an atomic level, in particular, these structures are not investigated by quantum-chemical methods. The present study is aimed at ab initio constructing atomic supercells based on graphene lithium-titanium phosphate

and vanadium-lithium phosphate as well as estimating their electron-energy parameters: formation energy, a Fermi level, a density of electron states, quantum capacitance and a surface charge density.

### 1. Research methods

The studied structures were atomistically simulated by a DFT method (Density Functional Theory) as part of the gradient approximation (GGA) with the exchange and correlation functional in the PBE version [10] in the Siesta software package [11]. Dispersion interactions were taken into account by the Grimme correction DFT-D2 [12]. The Li, P, V atoms were simulated in the DZP basis, while the O and C atoms were simulated in the lightweight DZ basis. This is due to the fact that taking into account polarization orbitals by the DZP basis for the O and C atoms contributes only 4% to the total charge of the atoms, while for the atoms Li, Ti, P, V this accounting contributes already about 25% to the total charge. Integration over the irreducible part of the Brillouin zone was performed by a Monkhorst-Pack method on grids of  $k$ -points  $12 \times 12 \times 1$  for 2D-films. Convergence with respect to a force affecting the atom did not exceed 0.05 eV/Å. The density of electronic states (DOS) was plotted based on the eigenvalue matrix obtained by solving the stationary Schrödinger equation. When constructing the DOS, Gaussian distributions with a broadening of 0.05 were used.

Energy of formation of the composite between graphene, lithium-titanium phosphate and vanadium-lithium phosphate

was calculated by a classic formula:

$$Eb(G/LTP/LVP) = E(G/LTP/LVP) - E(G) - E(LTP) - E(LVP),$$

where  $E(G/LTP/LVP)$  is full energy of the composite,  $E(G)$ ,  $E(LVP)$  and  $E(LTP)$  are full energies of graphene, lithium titanate and lithium-vanadium oxide in an isolated state, respectively.

The DFT method in an approximation of localized molecular orbitals implies that basis functions are atom-centered. It means that a number of electrons belonging to the this atom can be found by summing all the basis functions. According to the Mulliken formula, the charge on the atom  $A$  can be found by the formula

$$q_A = Z_A - \sum_{\mu \in A} (PS)_{\mu\mu},$$

where  $Z_A$  is an atomic charge of a nucleus,  $P$  is a density matrix,  $S$  is an overlap matrix,  $\mu$  is a atomic orbital basis index [13].

Quantum capacitance (often referred to as „differential quantum capacitance“), [F/g] for a stationary structure depending on the applied voltage  $\mu$ , [V], corresponding to the Fermi level shift  $E_F$  can be obtained based on the DOS graph [14]:

$$C_q^{\text{diff}} = \frac{e^2}{S} \int_{-\infty}^{+\infty} D(E) F_T(E - \mu) dE,$$

where  $S$  is an area of the structure surface, [cm<sup>2</sup>],  $D$  is an area under the DOS graph in the considered energy range, [eV<sup>-1</sup>·eV],  $e$  — the elementary charge, [C],  $F_T(E)$  is a thermal broadening function, [eV<sup>-1</sup>]. The differential quantum capacitance reflects variation of the accumulated charge taking into account an applied potential corresponding to the Fermi level. As proposed by S. Luriy, in the chemical current sources with low-dimensional structures as electrodes, the quantum capacitance limits full capacitance of the structure  $C_T$  along with geometrical capacitance  $C_D$  [15]:

$$\frac{1}{C_T} = \frac{1}{C_q^{\text{diff}}} + \frac{1}{C_D}.$$

The surface charge density ( $C/g$ ) can be found as an integral of a curve of differential quantum capacitance:

$$Q = \int_0^{\mu} C_q^{\text{diff}} d\mu.$$

It is important to calculate the surface charge density for predicting an electrode type in one electrolyte or another. A criterion of determining the electrode type is a ration of absolute values of the maximum surface charge density at negative voltage ( $\sigma_a$ ) to the maximum surface charge density at positive voltage ( $\sigma_b$ ) within a range of electrolyte's

working potentials. If  $\sigma_a/\sigma_b > 1.05$ , then the materials is more suitable for the anode, if  $\sigma_a/\sigma_b < 0.95$ , it is more suitable for the cathode, and when  $0.95 < \sigma_a/\sigma_b < 1.05$ , the material is a symmetrical electrode [7].

## 2. Results

The present study has considered the supercells of the 2D-films of the composites based on graphene (G), LTP and LVP, whose designations correspond to a sequence of their layout: LTP/G/LVP, LVP/LTP/G and LTP/LVP/G (Fig. 1). Table 1 shows optimal translation vectors  $L_x$  and  $L_y$  both for the produced 2D-films of the composites as well as their isolated components (the translation vector along the axis perpendicular to the film plane,  $L_y$ , was pre-defined to be 100 Å in order to exclude interlayer interaction after translation) as well as the coefficients of compression/tension of the translation vectors in relation to the isolated state ( $\varepsilon_x$  and  $\varepsilon_y$ ). As it is clear from Table 1, the greatest deformations belong to graphene, which is tensioned along a zigzag direction by 12.87%–13.09%. Sizes of the LVP cell vary within the range 0.23%–1.89%, whereas sizes of the LTP cell remain almost unchanged. We note that all the considered composites are formed with energy release. The highest formation energy corresponds to the LTP/LVP/G 2D-film (–7.02 eV), while the least one

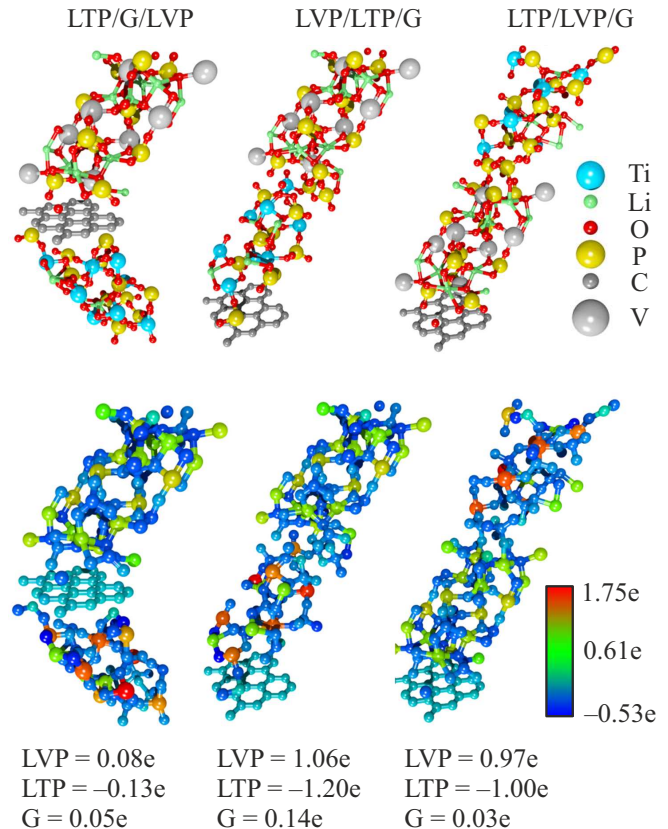


**Figure 1.** Atomic supercells of the composites LTP/G/LVP, LVP/LTP/G and LTP/LVP/G as well charge distribution on atoms.

**Table 1.** Boundary conditions of the 2D-films of the composites based on graphene, lithium-titanium phosphate and vanadium-lithium phosphate as well as coefficients of compression/tension of translation vectors in relation to the isolated state

Structure	$L_x, \text{Å}$	$L_y, \text{Å}$	$\varepsilon_x(\text{Gr}), \%$	$\varepsilon_y(\text{Gr}), \%$	$\varepsilon_x(\text{LTP}), \%$	$\varepsilon_y(\text{LTP}), \%$	$\varepsilon_x(\text{LVP}), \%$	$\varepsilon_y(\text{LVP}), \%$
Graphene	7.38	8.52						
LTP	8.49	8.59						
LVP	8.63	8.62						
LTP/G/LVP	8.48	8.59	12.97	0.82	0.12	0.00	1.74	0.35
LVP/LTP/G	8.49	8.60	13.09	0.93	0.00	0.12	1.65	0.23
LTP/LVP/G	8.47	8.57	12.87	0.58	0.24	0.23	1.89	0.58

corresponds to the LTP/G/LVP film ( $-0.19 \text{ eV}$ ). Energy of formation of LVP/LTP/G is ( $-4.83 \text{ eV}$ ).

Redistribution of an absolute charge in the produced 2D-films significantly varies depending on the layout (Fig. 1). In the LTP/G/LVP composite, the components remain almost electroneutral: the total charge on the graphene atoms is  $0.05e$ , and it is  $0.08e$  on the LVP atoms and  $-0.13e$  on the LTP atoms. It can be concluded that in the LTP/G/LVP system a graphene sheet prevents charge exchange between LTP and LVP. Thus, interaction of the components in this system is the least, thereby explaining the low formation energy. In the cases of LVP/LTP/G and LTP/LVP/G, the main charge transfer occurs between phosphates. The maximum charge transfer is observed in the case when a central component of the system is the LTP cell: in this case the LVP cell accepts the charge of  $1.06e$  and the graphene cell accepts the charge of  $0.14e$ . When there is the LVP cell between graphene and LTP, LTP acts as a charge donor, but the total charge imparted to the adjacent system components is  $-1e$ . Total redistribution of the charge per the system atom types is shown in Table 2. As it is clear from Table, the atoms of phosphorous and oxygen expectedly act as the charge donors. At the same time, the largest charge is lost by oxygen atoms from the LTP cell painted in various red shades at a lower part of Fig. 1.

The graphs of the DOS and the partial DOS are shown in Fig. 2. All the obtained Fermi levels of the considered structures are within a range of the Fermi levels of the components (Table 3). The least Fermi level corresponds to the LTP/G/LVP system ( $-6.11 \text{ eV}$ ), while for the other structures the Fermi level is shifted to the right. The DOS graphs for all the structures are similar and different only by diversity of the peaks to the right of the Fermi level (Fig. 3, a). Each structure at the Fermi level exhibits a peak of the value of about  $40 \text{ eV}^{-1}$ , which is mainly contributed by  $d$ -orbitals of vanadium. An energy gap to the left of the Fermi level is closed by a contribution by the partial DOSes of carbon atoms.

Fig. 3, b shows dependences of differential quantum capacitance on the applied voltage for the film composites LVP/G/LTP, G/LVP/LTP and G/LTP/LVP. The largest

**Table 2.** Redistribution of the charge on the atoms and the components of the 2D-films LTP/Gr/LVP, LVP/LTP/Gr and LTP/LVP/Gr

Atom	Charge, e		
	LTP/G/LVP	LVP/LTP/G	LTP/LVP/G
Li	13.57	13.68	13.67
Ti	12.32	12.47	12.56
C	0.05	0.14	0.03
P	$-5.77$	$-6.03$	$-6.19$
V	8.52	8.47	8.38
O	$-28.69$	$-28.47$	$-28.46$

value of quantum capacitance at  $0 \text{ V}$  is observed for the LTP/G/LVP composite ( $1161.35 \text{ F/g}$ ), so is the least one for the LVP/LTP/G composite ( $1022.17 \text{ F/g}$ ). All the considered structures are characterized by sharp reduction of quantum capacitance when voltage decreases from  $0$  to  $-0.3 \text{ V}$ . It is clearly seen in Fig. 3, c that the graphs of the surface charge density in a dependence on the applied voltage are almost the same. Analyzing the values of the surface charge density in the ranges of the electrolytes working potentials as exemplified by the aqueous and non-aqueous liquid systems, it can be concluded that all the composites considered in the study are pronounced cathodes ( $\sigma_a/\sigma_b < 0.95$ ) (Table 4).

## Conclusion

We have ab initio optimized the supercells of the composite 2D-films based on graphene, lithium-titanium phosphate and vanadium-lithium phosphate with various packaging types. It is found that the most energetically profitable is synthesis of the LTP/LVP/G structure: its formation results in release of a heat amount of  $-7.02 \text{ eV}$ . It is explained by the most noticeable redistribution of the charge between the phases inside the composite: the

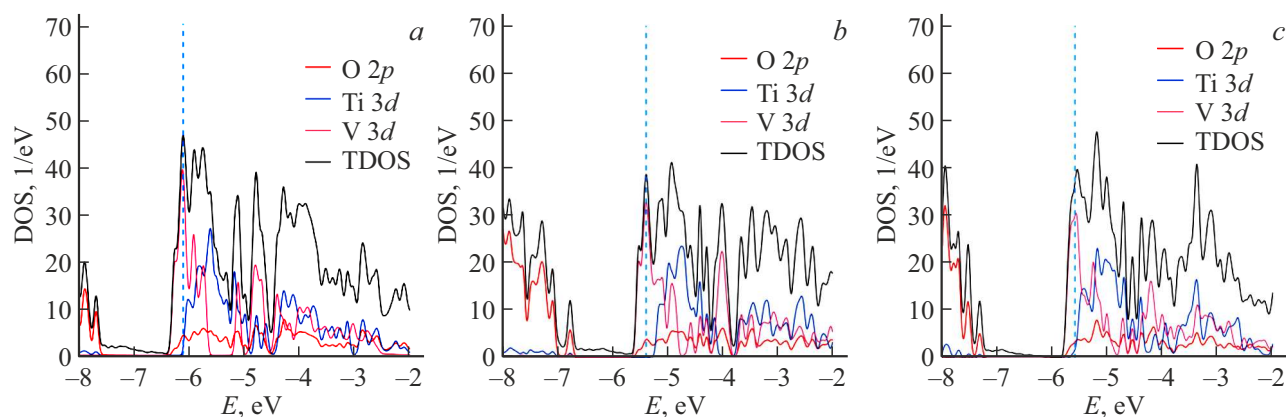


**Figure 2.** Graphs of the DOSes and the partial DOSes for the composites: *a* — LVP/G/LTP; *b* — G/LVP/LTO; *c* — G/LTP/LVP.

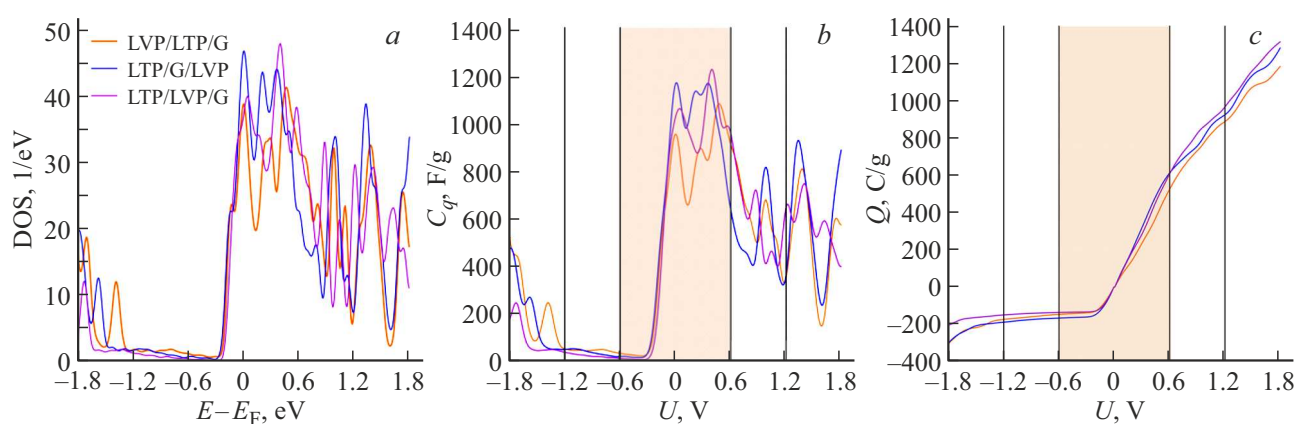


**Figure 3.** Electron-energy characteristics of the composites LVP/G/LTP, G/LVP/LTP and G/LTP/LVP: *a* — the DOS; *b* — the differential quantum capacitance; *c* — the surface charge density.

**Table 3.** Electron-energy characteristics of the 2D-films based on graphene, lithium-titanium phosphate and lithium-vanadium phosphate as well as their components separately

Structure	Fermi level, eV	Bonding energy, eV	DOS (Fermi level), eV <sup>-1</sup>	$C_q^{\text{diff}}$ (Fermi level), F/g
Graphene	-4.54		0.00	0.00
LTP	-7.35		0.00	0.00
LVP	-5.15		69.73	3505.13
LTP/G/LVP	-6.11	-0.19	46.58	1161.35
LVP/LTP/G	-5.39	-4.83	38.62	1022.17
LTP/LVP/G	-5.59	-7.02	36.95	951.63

LTP cell acts as a charge acceptor and accepts  $-1.20e$  received from the LVP cell ( $1.06e$ ) and the graphene cell ( $0.14e$ ). The least redistribution of the charge and formation energy corresponds to the LTP/G/LVP composite, since in this system the graphene cell is between phosphates and prevents their active interaction.

The largest quantum capacitance at the Fermi level is demonstrated by the LTP/G/LVP composite (1161.35 F/g),

so is the slightly lower one by LVP/LTP/G (1022.17 F/g), and so is the least one by LTP/LVP/G (951.63 F/g). At the same time, transformation of the quantum capacitance curve is the same for all the composites: when voltage decreases from 0 to  $-2$  V the values of quantum capacitance sharply decrease; when voltage increases from 0 to 3 V they decrease not so much. The dependence of the surface charge density was analyzed to show that the considered

**Table 4.** Maximum values of the surface charge density of the composites LVP/G/LTP, G/LVP/LTP and G/LTP/LVP in the ranges of the electrolytes working potentials

Composite	Aqueous medium (−0.6; 0.6 V)				Non-aqueous medium* (−1.2; 1.2 V)			
	$\sigma_a$ , C/g	$\sigma_b$ , C/g	$\sigma_a/\sigma_b$	Electrode	$\sigma_a$ , C/g	$\sigma_b$ , C/g	$\sigma_a/\sigma_b$	Electrode
LTP/G/LVP	166.81	616.44	0.27	Cathode	189.19	927.37	0.20	Cathode
LVP/LTP/G	146.83	530.67	0.28	Cathode	174.13	890.75	0.19	Cathode
LTP/LVP/G	136.34	613.26	0.22	Cathode	150.15	971.67	0.15	Cathode

*Note.* \* The non-aqueous medium is understood to be any liquid electrolyte that is applied or considered for application in the lithium-ion accumulators and is either a lithium salt solution (LiPF<sub>6</sub>, LiBF<sub>4</sub>, LiClO<sub>4</sub>, etc.) in a mixture of organic solvents or an ionic liquid. The main difference from the aqueous medium is an extended range of potentials of oxidation-reduction stability.

composites were cathodes, if electrolytes are both aqueous as well as non-aqueous liquid systems.

It is found that the total Fermi level varies in a dependence on a sequence of „packaging“ of the three phases. The said packaging can be correlated to formation of core-shell structures and contact of an external shell with the third phase. The higher Fermi level among the considered options for the LVP/LTP/G sequence (−5.39 eV) shall correspond to improvement of conditions for transferring an electron from the composite to a current collector, i.e. to its oxidation. The lowest Fermi level for the LTP/G/LVP sequence (−6.11 eV) corresponds to the largest difficulties of oxidation. The next important stage of the study is to trace a pattern of variation of the Fermi level and quantum capacitance when extracting lithium from the variously-packaged composites. Such calculations can initiate experiments of comparing properties of the three-phase composites with a variously-packaged order.

## Funding

The study was funded by the Russian Science Foundation (project No. 25-22-00290).

## Conflict of interest

The authors declare no conflict of interest.

## References

- [1] C. Liu, R. Massé, X. Nan, G. Cao. *Energy Storage Mater.*, **4**, 15 (2016). DOI: 10.1016/j.ensm.2016.02.002
- [2] A.V. Ivanishchev, A.V. Ushakov, I.A. Ivanishcheva, A.V. Churikov, A.V. Mironov, S.S. Fedotov, N.R. Khasanova, E.V. Antipov. *Electrochim. Acta*, **230**, 479 (2017). DOI: 10.1016/j.electacta.2017.02.009
- [3] J. Xiao, B. Zhang, J. Liu, X. He, Zh. Xiao, H. Qin, T. Liu, Kh. Amine, X. Ou. *Nano Energy*, **127**, 109730 (2024). DOI: 10.1016/j.nanoen.2024.109730
- [4] Z. Guo, X. Qin, Y. Xie, Ch. Lei, T. Wei, Y. Zhang. *Chem. Phys. Lett.*, **806**, 140010 (2022). DOI: 10.1016/j.cplett.2022.140010
- [5] A.V. Ushakov, S.V. Makhov, N.A. Gridina, A.V. Ivanishchev, I.M. Gamayunova. *Monatsh Chem.*, **150**, 499 (2019). DOI: 10.1007/s00706-019-2374-4
- [6] S. Yu, A. Mertens, R. Schierholz, X. Gao, Ö. Aslanbas, J. Mertens, H. Kungl, H. Tempel, R.A. Eichel. *J. Electrochem. Soc.*, **164** (2), A370 (2017). DOI: 10.1149/2.1151702jes
- [7] H. Wang, H. Zhang, Yi. Cheng, K. Feng, X. Li, H. Zhang. *Electrochim. Acta*, **278**, 279 (2018). DOI: 10.1016/j.electacta.2018.05.047
- [8] X. Li, N. Wang, T. Su, Y. Chai. *Appl. Surf. Sci.*, **601**, 154285 (2022). DOI: 10.1016/j.apsusc.2022.154285
- [9] X. Wang. *Int. J. Electrochem. Sci.*, **16** (11), (2021). DOI: 10.20964/2021.11.52
- [10] J.P. Perdew, K. Burke, M. Ernzerhof. *Phys. Rev. Lett.*, **77** (18), 3865 (1996). DOI: 10.1103/PhysRevLett.77.3865
- [11] J.M. Soler, E. Artacho, J.D. Gale, A. García, J. Junquera, P. Ordejón, D. Sánchez-Portal. *J. Phys. Condens. Matter*, **14**, 2745 (2002). DOI: 10.1088/0953-8984/14/11/302
- [12] S. Grimme. *J. Comput. Chem.*, **27**, 1787 (2006). DOI: 10.1002/jcc.20495
- [13] R.S. Mulliken. *J. Chem. Phys.*, **23** (10), 1833 (1955). DOI: 10.1063/1.1740588
- [14] V.V. Shunaev, A.A. Petrunin, A.V. Ushakov, O.E. Glukhova. *Tech. Phys.*, **94** (3), 372 (2024). DOI: 10.61011/JTF.2024.03.57374.314-23
- [15] S. Luryi. *Appl. Phys. Lett.*, **52**, 501 (1988). DOI: 10.1063/1.99649

*Translated by M.Shevelev*